Mehdi ALEMI-ROSTAMI, Adib ABRISHAMIFAR

Iran University of Science and Technology (IUST) (1), Iran University of Science and Technology (IUST) (2)

Speed Sensorless Control of Induction Motor Based on a Non-Linear Flux and Speed Observer with Parameters Estimation and Considering Iron Loss

Abstract. In this paper, a control method is presented for induction motor which offers high efficiency and high dynamics even considering the influences of iron loss. Recently, research to consider the influences of iron loss has been made in the vector control of an induction motor. Vector control method is a quite complex task which demands precise information about the rotor speed and the position of the magnetic flux. The vector control method presented in this paper, estimates both rotor speed and amplitude magnetic flux rotor. However, there are also applications in which even speed sensors should be omitted. In this method, three-phase motor currents and DC link voltage are measured by means of a nonlinear observer and considering the Lyapunov function for current error, motor parameters, rotor shaft and position of flux are estimated. To stabilize the control system, the Lyapunov function for error, is used. Then, using the genetic algorithm, the value of controlling coefficients their and general effects on system's behavior are obtained. The simulation and experimental results confirm the resistant performance and the proper dynamic efficiency of this method.

*Streszczenie. W artykule przedstawiono algorytm sterowania maszyną indukcyjną, uwzględniający straty w żelazie. Sterowanie opiera się na bezczujnikowym pomiarze prędkości obrotowej, przy pomocy obserwatora. Korzystając z pomiarów prądów fazowych i napięcia DC-link, z funkcji Lyapunov'a wyznaczana jest prędkość i strumień wirnika. Implementacja algorytmu genetycznego pozwoliła na ocenę wpływu współczynników regulacji na odpowiedź układu. Przedstawiono wyniki symulacyjne i eksperymentalne. (**Sterowanie maszyną indukcyjną z bezczujnikowym pomiarem prędkości obrotowej – nieliniowy obserwator strumienia i prędkości z estymacją parametrów i uwzględnieniem strat w żelazie**).*

Keywords: iron loss, direct-field-oriented control, speed-sensorless contro,l Lyapunov function,.
Słowa kluczowe: straty w żelazie, bezpośrednie sterowanie polowe, sterowanie bezczujnikowe, funkcja Lapunov'a.

Introduction

Because of the vector control method's robust structure and high efficiency and high dynamics in induction motors, it is widely used in industry [1],[2]. In the previous conventional vector control methods, losses are not considered which result in improper estimation of rotor flux, thus the output torque would be far from its reference [3]. Because of energy is expensive and has many industrial and domestic usages, various methods were presented to reduce the consumed energy in motors and drives [4]. In industrial application, there is a control method which can be used in very high and very low speeds and in a vast range of dynamics in full load and in a vast range of speed stability [5].

The price of control system and drive must be reduced as possible. Speed sensor is a very expensive element comparing to other elements in circuit and by eliminating it, we can reduce the final price of drive system [6]-[7]. Therefore, control method must be estimated the speed motor by means of other measurable parameters. Various methods were presented previously [8]. The most common method is the Kalman filter. The other method is to find the state observer using structures like Luenberger [9]. These methods require detailed information about the model to properly estimate the unknown parameters. In case of drive system, the model parameters change during system operation, also the changes in motor speed are widely ranged. In addition, load dynamic is usually unknown. All of these factors reduce the performance of the common methods [10]-[14].

Generally, in the field-oriented control of an induction machine, it is assumed that iron loss may be neglected. Unfortunately, in practice, iron loss makes the output torque different from the reference torque, and the performance is deteriorated. To solve the problems caused by iron loss, the effects of iron loss in the vector-controlled induction motor have been investigated and compensated for in the last several years and considerable effectiveness has been achieved in performance and efficiency.

This paper investigates the effects of iron loss in the direct stator-flux-oriented control system of an induction motor, and proposes a control algorithm considering iron loss. The iron loss is modeled by equivalent iron loss resistance in parallel with the magnetizing inductance. Then, a non-linear observer is used to estimate the rotor flux and speed and parameters dynamics are estimated during system operation. A Lyapunov function is presented for an observer error model to ensure the control system stability during the system operation. In addition to the estimation of parameters are used Lyapunov function and error function. The motor parameters are obtained by tuning these parameter coefficients [15],[16]. To tune these coefficients, firstly by using of the observer gain tuning section, the parameters effect on control system are obtained and its proper domain their determined [17]-[19]. Then, by means of genetic algorithm, an acceptable value is presented for each of parameters [20]-[23]. The effectiveness of the proposed method is verified by simulation and experimental results.
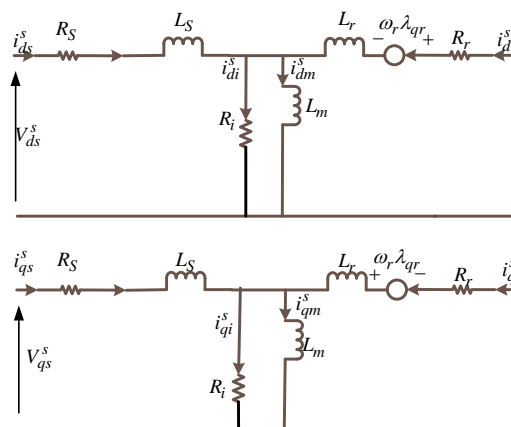

Fig. 1. Induction motor d–q equivalent circuit considering iron loss.

Ac Induction Motor

Fig. 1 shows the equivalent circuit of an induction motor considering iron loss in the rotating d–q stationary frame of reference frame. To perform direct-field-oriented control, it is necessary to obtain an accurate value for the rotor flux.

Furthermore, changes in the motor parameter are a serious problem. To solve these problems, this system employs a nonlinear observer that takes core loss into account. Equations (1) to (10) give the state and output equations for a stationary frame of reference. The term is an approximate expression

(1)

$$\begin{cases} \dot{X} = AX + Bu \\ Y = CX \end{cases}$$

$$X = [i_{ds}, i_{qs}, \lambda_{dr}, \lambda_{qr}]^T; \qquad u = [V_{ds}, V_{qs}]^T$$

$$A = \begin{bmatrix} a_{11}, 0, a_{13}, a_{14} \\ 0, a_{11}, -a_{14}, a_{13} \\ a_{31}, 0, a_{33}, a_{34} \\ 0, a_{31}, -a_{34}, a_{33} \end{bmatrix}; \qquad B = \begin{bmatrix} b_1, 0 \\ 0, b_1 \\ 0, 0 \\ 0, 0 \end{bmatrix}$$

$$C = eye(4)$$

where

(2) $$a_{11} = -(\frac{R_S}{\sigma L_s} + \frac{(1+\sigma)R_r}{\sigma L_r})$$

(3) $$a_{13} = \frac{L_m R_r}{\sigma L_s L_r^2} - \frac{(L_r - sL_m)R_i}{\sigma L_s L_r^2}$$

(4) $$a_{14} = -\frac{\omega_r L_m}{\sigma L_s L_r}$$

(5) $$a_{31} = -\frac{L_m R_r}{L_r}$$

(6) $$a_{33} = -(\frac{R_r}{L_r} + \frac{sR_i}{L_r})$$

(7) $$a_{34} = +\omega_r$$

(8) $$b_1 = \frac{1}{\sigma L_s}$$

(9) $$s = \frac{\omega_e - \omega_r}{\omega_e}$$

(10) $$\sigma = 1 - \frac{L_m^2}{L_s L_r}$$

Here the superscript of "s" refers to the stationary reference. The Flux equations, motor torque equation and mechanical basis equation are as

(11) $$\lambda_{ds}^s = L_m i_{dm}^s + l_{1s} i_{ds}^s$$

(12) $$\lambda_{qs}^s = L_m i_{qm}^s + l_{1s} i_{qs}^s$$

(13) $$\lambda_{dr}^s = L_m i_{dm}^s + l_{1r} i_{dr}^s$$

(14) $$\lambda_{qr}^s = L_m i_{qm}^s + l_{1r} i_{qr}^s$$

(15) $$L_s = L_{1s} + L_m$$

(16) $$L_r = L_{1r} + L_m$$

(17) $$T_e = \frac{3}{2} z_p (\lambda_{qr}^s i_{dr}^s - \lambda_{dr}^s i_{qr}^s)$$

(18) $$j\frac{d\omega_m}{dt} = T_e - T_l$$

Here, R_s is stator resistance, R_r is rotor resistance, L_m, magnet inductance, L_s is stator inductance, L_r is rotor inductance, ω_m is the Shaft Speed, ω_e stator frequency, z_p is pair pole, T_e is motor torque, T_l is load torque, V_{ds} and V_{qs} are the d- and q-axes stator voltages, i_{ds} and i_{qs} are the d- and q-axes stator currents, i_{dr} and i_{qr} are the d- and q-axes rotor currents, λ_{ds} and λ_{qs} are the d- and q-axes stator fluxes, λ_{dr} and λ_{qr} are the d- and q-axes rotor fluxes, λ_{dm} and λ_{qm} are the d- and q-axes air-gap fluxes, i_{di} and i_{qi} are the d- and q–axes currents flowing and R_i is the equivalent iron loss resistance, are defined. The current equations are given as

(19) $$i_{ds} + i_{dr} = i_{dm} + i_{di}$$

(20) $$i_{qs} + i_{qr} = i_{qm} + i_{qi}$$

The measurement of core loss resistance can be done by means of the unload test with stator supply sinusoidal voltage or PWM. The PWM voltage source is known to cause a significant increase in total iron loss, compared with a purely sinusoidal supply. However, the iron loss produced by higher order harmonics of the PWM voltage supply has no impact on accuracy of the vector control. Accordingly, the component of iron loss that is relevant for detuning studies is only the first harmonic component, which represents the equivalent iron loss resistance in the modeling. In addition, the iron loss of the first order harmonic is almost equal to that of sinusoidal voltage supply in no load test, the source power is equal to the copper losses, core losses and iron losses; mechanical losses in unload test are very low. The copper losses are obtained by measuring stator current and stator resistance. The test results for the induction motor shown in Table I are shown in Fig. 2 motor parameters are available in Appendix. It can be seen that the equivalent iron loss Ri resistance is a function of operating frequency.
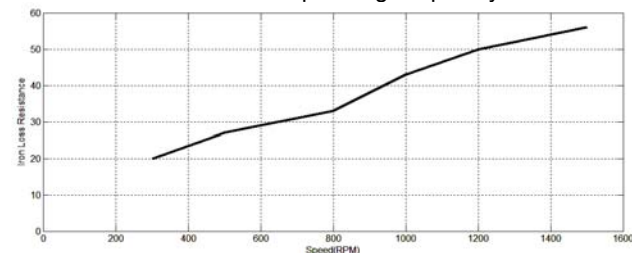

Fig. 2. Equivalent iron loss resistance respect to speed.

After manipulating, assuming that the flux and current improved equations are defined as,

(21) $$y_1 = \varepsilon_i i_{ds}^s , \; y_2 = \varepsilon_i i_{qs}^s , \; y_3 = \varepsilon_\lambda \lambda_{dr}^s , \; y_4 = \varepsilon_\lambda \lambda_{qr}^s$$

$$U_1 = V_{ds}^s , \; U_2 = V_{qs}^s , \; \varepsilon_i = \sigma L_s , \; \varepsilon_\lambda = \frac{L_m}{L_r}$$

The machine equations can be transferred into a more suitable form

(22) $$\frac{dy_1}{dt} = -a_1 y_1 + a_2 y_3 + z_p \omega_m y_4 + U_1$$

(23) $$\frac{dy_2}{dt} = a_1 y_1 - z_p \omega_m y_3 + a_2 y_4 + U_2$$

(24) $$\frac{dy_3}{dt} = a_3 y_1 - a_4 y_3 - z_p \omega_{m4} y_4$$

(25) $$\frac{dy_4}{dt} = a_3 y_2 +_p \omega_m y_3 + a_4 y_4$$

where,

(26) $$a_1 = \frac{R_s}{\delta L_s} + \frac{(1+\delta)R_r}{\delta L_r}$$

(27) $$a_2 = \frac{R_r}{L_r} - \frac{R_i(L_r - sL_m)}{L_m L_r}$$

(28)
$$a_3 = \frac{L_m^2 R_r}{L_r^2 \delta L_s}$$

(29)
$$a_4 = \frac{R_r}{L_r} + \frac{s R_m}{L_r}$$

Purposed Observer

The proposed control structure is shown in Fig. 3. Observer states can be determined by measuring the stator current, knowing the inverter switches, estimation of rotor flux and by using them we can find the motor shaft speed. Meanwhile, we can determine the observer parameters model.

The state observer structure is suggested on the basis of machine model, where "~" is the parameter estimation sign.

(30)
$$\frac{d\tilde{y}_1}{dt} = -\tilde{a}_1 \tilde{y}_1 + \tilde{a}_2 \tilde{y}_3 + z_p \tilde{\omega}_m \tilde{y}_4 + U_1 + \delta_1$$

(31)
$$\frac{d\tilde{y}_2}{dt} = -\tilde{a}_1 \tilde{y}_2 + z_p \tilde{\omega}_m \tilde{y}_3 + \tilde{a}_2 \tilde{y}_4 + U_1 + \delta_2$$

(32)
$$\frac{d\tilde{y}_3}{dt} = \tilde{a}_3 \tilde{y}_1 - \tilde{a}_4 \tilde{y}_3 - z_p \tilde{\omega}_m \tilde{y}_4$$

(33)
$$\frac{d\tilde{y}_4}{dt} = +\tilde{a}_3 \tilde{y}_2 + z_p \tilde{\omega}_m \tilde{y}_3 - \tilde{a}_4 \tilde{y}_4$$
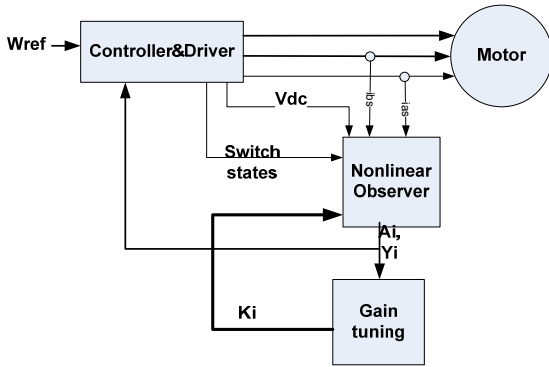

Fig. 3. Speed and flux observer structure.

State observer can estimate by measuring the stator voltage and current. Also, the coefficients a_i must be updated. δ_1 and δ_2 are error correction based on the stator current error there are referred to nonlinear gain observers. Here, the error amounts are expressed as,

(34)
$$\Delta y_i = \tilde{y}_i - y_i \quad ; i = 1, 2, 3, 4$$

(35)
$$\Delta a_i = \tilde{a}_i - a_i \quad ; i = 1, 2, 3, 4, 5$$

Error variation in state values is defined from equations (34) and (35) as,

(36)
$$\frac{d\Delta y_i}{dt} = \frac{d\tilde{y}_i}{dt} - \frac{dy_i}{dt} \quad ; i = 1, 2, 3, 4$$

By equations (33)-(35), we can obtain the error dynamics of rotor flux and stator current as

(37)
$$\frac{d\Delta y_1}{dt} = +\Delta a_1 \tilde{y}_1 + (\tilde{a}_1 - \Delta a_1)\Delta y_1 + \Delta a_2 \tilde{y}_3 + (\tilde{a}_2 - \Delta a_2)\Delta y_3$$
$$+ z_p \Delta \omega_r \tilde{y}_4 + (z_p \tilde{\omega}_r - \Delta z_p \omega_r)\Delta y_4 + \delta_1$$

(38)
$$\frac{d\Delta y_2}{dt} = +\Delta a_1 \tilde{y}_2 + (\tilde{a}_1 - \Delta a_1)\Delta y_2 - \Delta z_p \omega_r \tilde{y}_3$$
$$-(z_p \tilde{\omega}_r - \Delta z_p \omega_r)\Delta y_3 + \Delta a_2 \tilde{y}_4 + (\tilde{a}_2 - \Delta a_2)\Delta y_4 + \delta_2$$

(39)
$$\frac{d\Delta y_3}{dt} = \Delta a_3 \tilde{y}_1 + (\tilde{a}_3 - \Delta a_3)\Delta y_1 + \Delta a_4 \tilde{y}_3 + (\tilde{a}_4 - \Delta a_4)\Delta y_3$$
$$- z_p \Delta \omega_r \tilde{y}_4 - (z_p \tilde{\omega}_r - \Delta z_p \omega_r)\Delta y_4$$

(40)
$$\frac{d\Delta y_4}{dt} = \Delta a_3 \tilde{y}_2 + (\tilde{a}_3 - \Delta a_3)\Delta y_2 + z_p \Delta \omega_r \tilde{y}_3$$
$$+(z_p \tilde{\omega}_r - \Delta z_p \omega_r)\Delta y_3 - \Delta a_4 \tilde{y}_4 - (\tilde{a}_4 - \Delta a_4)\Delta y_4$$

Equations (37) to (40), are presented as system error

equations. Considering that the estimation error must be minimized, δ_1 and δ_2 values are presented by stator current error. In order to set the current error to zero in respect of time changes, the Lyapunov function must include an integral statement of current error. For this reason, the auxiliary variable, β_1 and β_2 are defined as current error integral as,

(41)
$$\beta_1 = \int \Delta i_{sd}' dt$$

(42)
$$\beta_2 = \int \Delta i_{sq}' dt$$

In order to set the current error to zero in respect of time, it is required to consider the error as

(43)
$$\frac{d\beta_1}{dt} = \gamma_1 - m_1 \beta_1$$

(44)
$$\frac{d\beta_2}{dt} = \gamma_2 - m_2 \beta_2$$

m_1 and m_2 are constant gains. In this case, the error system will be stable. The Lyapunov function is defined as

(45)
$$V = \frac{1}{2}\beta_1^2 + \frac{1}{2}\beta_2^2 + \frac{1}{2}\gamma_1^2 + \frac{1}{2}\gamma_2^2 + \frac{1}{2}\Delta y_3^2$$
$$+ \frac{1}{2}\Delta y_4^2 + \frac{1}{2}\frac{(\Delta a_1)^2}{k_1} + \frac{1}{2}\frac{(\Delta a_2)^2}{k_2} + \frac{1}{2}\frac{(\Delta a_3)^2}{k_3}$$
$$+ \frac{1}{2}\frac{(\Delta a_4)^2}{k_4} + \frac{1}{2}\frac{(\Delta \omega)^2}{k_\omega}$$

The system is stable, where

(46)
$$\frac{d}{dt}V < 0$$

In the following, time derivation of Lyapunov function is calculated.

(47)
$$\frac{d}{dt}V = \beta_1 \Delta y_1 + \beta_2 \Delta y_2 - a_1(\eta_1^2 + \eta_2^2) - a_3(X_1^2 + X_2^2)$$
$$+ \gamma_1 \left\{ -\Delta y_1(-a_1 - a_2 + m_1 + m_1) - \Delta y_2(+z_p \omega_m) + \delta_1 \right\}$$
$$+ \gamma_2 \left\{ -\Delta y_1(-z_p \omega_m) - \Delta y_2(-a_1 - a_2 + m_1 + m_1) + \delta_2 \right\}$$
$$+ \Delta a_1 \left\{ \frac{\frac{d\Delta a_1}{dt}}{k_1} - \gamma_1 \tilde{y}_1 - \gamma_2 \tilde{y}_2 + \Delta y_1 \gamma_1 + \Delta y_2 \gamma_2 \right\} +$$
$$\Delta a_2 \left\{ \frac{\frac{d\Delta a_2}{dt}}{k_2} + \gamma_1 \tilde{y}_3 + \gamma_2 \tilde{y}_4 - \Delta y_3 \gamma_1 - \Delta y_4 \gamma_2 \right\}$$

$$+ \Delta a_3 \left\{ \frac{\frac{d\Delta a3}{k_3}}{dt} - \tilde{y}_1 \Delta y_1 - \tilde{y}_2 \Delta y_2 + \tilde{y}_1 (\Delta y_1)^2 + \tilde{y}_2 (\Delta y_2)^2 \right\}$$
$$+ \Delta a_4 \left\{ \frac{\frac{d\Delta a_4}{dt}}{k_4} + \tilde{y}_1 \Delta y_3 + \tilde{y}_2 \Delta y_3 - \tilde{y}_3 (\Delta y_1)^2 - \tilde{y}_4 (\Delta y_2)^2 \right\}$$
$$+ \Delta z_p \omega_m \left\{ \frac{\frac{d\Delta z_p \omega_m}{dt}}{k_\omega} + \gamma_1 \tilde{y}_4 - \gamma_2 \tilde{y}_3 + \Delta y_3 \tilde{y}_4 \atop -\Delta y_4 \tilde{y}_3 - \Delta y_4 \gamma_1 + \Delta y_3 \gamma_2 \right\}$$

Assuming δ_1 and δ_2 are defined as follow, by inserting the assumptions of equations (48) and (49) and also regarding that a_1 and a_3 are always negative, derivation of Lyapunov function can be obtained.

(48) $\delta_1 = \Delta y_1(-a_1 - a_2 + m_1 + m_1) + \Delta y_2(+z_p\omega_m) - (1 - m_1 m_2)\beta_1$

(49) $\delta_2 = \Delta y_1(-z_p\omega_m) + \Delta y_2(-a_1 - a_2 + m_1 + m_1) - (1 - m_1 m_2)\beta_2$

By negative derivation of Lyapunov function we can obtain the parameters equations as follows.

(50) $$\frac{d\Delta\tilde{a}_1}{dt} = -k_1\left\{-\gamma_1\tilde{y}_1 - \gamma_2\tilde{y}_2 + \Delta y_1\gamma_1 + \Delta y_2\gamma_2\right\}$$

(51) $$\frac{d\Delta\tilde{a}_2}{dt} = -k_2\left\{+\gamma_1\tilde{y}_3 + \gamma_2\tilde{y}_4 - \Delta y_3\gamma_1 - \Delta y_4\gamma_2\right\}$$

(52) $$\frac{d\Delta\tilde{a}_3}{dt} = -k_3\left\{-\tilde{y}_1\Delta y_1 - \tilde{y}_2\Delta y_2 + \tilde{y}_1(\Delta y_1)^2 + \tilde{y}_2(\Delta y_2)^2\right\}$$

(53) $$\frac{d\Delta\tilde{a}_4}{dt} = -k_4\left\{+\tilde{y}_1\Delta y_3 + \tilde{y}_2\Delta y_3 - \tilde{y}_3(\Delta y_1)^2 - \tilde{y}_4(\Delta y_2)^2\right\}$$

(54) $$\frac{d\Delta z_p\omega_m}{dt} = -k_\omega\left\{\begin{array}{l}+\gamma_1\tilde{y}_4 - \gamma_2\tilde{y}_3 + \Delta y_3\tilde{y}_4 \\ -\Delta y_4\tilde{y}_3 - \Delta y_4\gamma_1 + \Delta y_3\gamma_2\end{array}\right\}$$

Machine parameters and speed changes in respect of current and motor voltage changes, are very slow. Therefore

(55) $$\frac{d\Delta a_i}{dt} = \frac{d\tilde{a}_i}{dt} - \frac{da_i}{dt} = \frac{d\tilde{a}_i}{dt} \qquad \forall i = 1,2,3,4,5$$

The rotor magnetic-flux estimation error $\Delta\lambda'_{dr}$ and $\Delta\lambda'_{qr}$ are not known and cannot be measured. We have assumed that these values are equal to the negative value of modified stator current estimation error. Let us suppose that modified stator current and rotor magnetic-flux estimation errors are small and steady. Then

(56) $$\frac{d\Delta i'_{sd}}{dt} = -z_p\omega_m\Delta i'_{sq}$$

(57) $$\frac{d\Delta i'_{sq}}{dt} = +z_p\omega_m\Delta i'_{sd}$$

(58) $$\frac{d\Delta\lambda'_{sd}}{dt} = -z_p\omega_m\Delta\lambda'_{sq}$$

(59) $$\frac{d\Delta\lambda'_{sq}}{dt} = +z_p\omega_m\Delta\lambda'_{sd}$$

(60) $$\frac{d\Delta i'_{sd}}{dt} + \frac{d\Delta\lambda'_{sd}}{dt} = -z_p\omega_m(\Delta i'_{sq} + \Delta\lambda'_{sq})$$

(61) $$\frac{d\Delta i'_{sq}}{dt} + \frac{d\Delta\lambda'_{sq}}{dt} = +z_p\omega_m(\Delta i'_{sq} + \Delta\lambda'_{sd})$$

Substitution of (37) - (40) into (60) and (61) leads to

(62) $$\Delta i'_{sd} + \Delta\lambda'_{sd} = \frac{1}{-z_p\omega_m}\left((\Delta a_3 - \Delta a_1)i'_{sq} + (a_3 - a_1)i'_{sq} + \delta_2\right)$$

(63) $$\Delta i'_{sq} + \Delta\lambda'_{sq} = \frac{+1}{z_p\omega_m}\left((\Delta a_3 - \Delta a_1)i'_{sd} + (a_3 - a_1)i'_{sd} + \delta_1\right)$$

And if the estimation errors are small, we can write

(64) $$\Delta i'_{sd} + \Delta\lambda'_{sd} \simeq 0 \quad \Rightarrow \Delta\lambda'_{sd} \simeq -\Delta i'_{sd}$$

(65) $$\Delta i'_{sd} + \Delta\lambda'_{sd} \simeq 0 \quad \Rightarrow \Delta\lambda'_{sd} \simeq -\Delta i'_{sd}$$

The algorithm is only locally stable because we have to assume that the differences between real and estimated variable values are small. The complete algorithm can be summarized into the following equations:

(66) $$\Delta i_{sd} = \tilde{i}_{sd} - i_{sd}, \qquad \Delta i_{sq} = \tilde{i}_{sq} - i_{sq}$$

(67) $$y_1 = \varepsilon_i i_{sd}, \qquad y_2 = \varepsilon_i i_{sq}$$

(68) $$\tilde{y}_1 = \varepsilon_\lambda \tilde{i}_{sd} \qquad \tilde{y}_2 = \varepsilon_\lambda \tilde{i}_{sq}$$

(69) $$\Delta y_1 = \tilde{y}_1 - y_1 = \varepsilon_i(\tilde{i}_{sd} - i_{sd}) = \varepsilon_i\Delta i_{sd}$$

(70) $$\Delta y_2 = \tilde{y}_2 - y_2 = \varepsilon_i(\tilde{i}_{sq} - i_{sq}) = \varepsilon_i\Delta i_{sq}$$

(71) $$\Delta y_3 = \tilde{y}_3 - y_3 = -\Delta i_{sd} = -\Delta y_1$$

(72) $$\Delta y_4 = \tilde{y}_4 - y_4 = -\Delta i_{sq} = -\Delta y_4$$

(73) $$\frac{d\tilde{y}_1}{dt} = -\tilde{a}_1\tilde{y}_1 + \tilde{a}_2\tilde{y}_3 + z_p\tilde{\omega}_m\tilde{y}_4 + U_1 + \delta_1$$

(74) $$\frac{d\tilde{y}_2}{dt} = -\tilde{a}_1\tilde{y}_2 + z_p\tilde{\omega}_m\tilde{y}_3 + \tilde{a}_2\tilde{y}_4 + U_1 + \delta_2$$

(75) $$\frac{d\tilde{y}_3}{dt} = \tilde{a}_3\tilde{y}_1 - \tilde{a}_4\tilde{y}_3 - z_p\tilde{\omega}_m\tilde{y}_4$$

(76) $$\frac{d\tilde{y}_4}{dt} = +\tilde{a}_3\tilde{y}_2 + z_p\tilde{\omega}_m\tilde{y}_3 - \tilde{a}_4\tilde{y}_4$$

(77) $$\frac{d\tilde{a}_1}{dt} = -k_1\left\{-\gamma_1\tilde{y}_1 - \gamma_2\tilde{y}_2 + \Delta y_1\gamma_1 + \Delta y_2\gamma_2\right\}$$

(78) $$\frac{d\tilde{a}_2}{dt} = -k_2\left\{+\gamma_1\tilde{y}_3 + \gamma_2\tilde{y}_4 - \Delta y_3\gamma_1 - \Delta y_4\gamma_2\right\}$$

(79) $$\frac{d\tilde{a}_3}{dt} = -k_3\left\{-\tilde{y}_1\Delta y_1 - \tilde{y}_2\Delta y_2 + \tilde{y}_1(\Delta y_1)^2 + \tilde{y}_2(\Delta y_2)^2\right\}$$

(80) $$\frac{d\tilde{a}_4}{dt} = -k_4\left\{+\tilde{y}_1\Delta y_3 + \tilde{y}_2\Delta y_3 - \tilde{y}_3(\Delta y_1)^2 - \tilde{y}_4(\Delta y_2)^2\right\}$$

(81) $$\frac{d(z_p\omega_m)}{dt} = -k_\omega\left\{\begin{array}{l}+\gamma_1\tilde{y}_4 - \gamma_2\tilde{y}_3 + \Delta y_3\tilde{y}_4 \\ -\Delta y_4\tilde{y}_3 - \Delta y_4\gamma_1 + \Delta y_3\gamma_2\end{array}\right\}$$

In this case, the general algorithm of control is as (66) to (81). The behavior of the algorithm can be tuned by a set of parameters k_i and k_ω.

Observer Gain tuning

The proposed observer is a nonlinear system and it is very difficult to describe its dynamics analytically. That is why we have no general and automatic method for the observer-gain tuning at this time. However, it is possible to describe some guidelines for observer-gain tuning. One of the common methods to do that is using Kalman filter. But the Kalman filter requires information about noise signal and level to have a proper response which is not known here. Because in low speeds, the system noise is high and the motor parameters change during the system operation, the proper dynamic behavior is not obtained.

Considering the Lyapunov function and its time derivative, the only necessary condition for the proper performance of the observer, is positive gain. If we choose the small gain values, this slows the response and if we choose the big interests, this results in instability. Thus, the proper selection of the interest value in order to have a proper behavior is important.

The observer-parameter adaptation can be tuned by gains k_1, k_2, k_3, k_4 and k_5. It has been shown earlier that it is not usually possible to estimate rotor resistance by the presented algorithm. The gain k_1 should be set with respect to the stator thermal dynamics and the gain k_4 should be set with respect to the rotor thermal dynamics; the higher value it has, the faster stator-resistance changes due to temperature changes can be tracked. It is advisable to assume that Δk_2, Δk_3 is very low and set k_2, k_3 are very small value.

The last gain k_ω represents speed-tracking dynamics. A higher value can improve rotor-speed-change tracking. On the other hand, a high value of k_ω can cause poor performance in the low-speed region when speed information in the stator voltage and current measurement disappears, and the observer is then influenced mostly by noise signals.

Genetic algorithm

Genetic algorithm is a stochastic optimization method which works based on the natural generation mechanism. This method finds the optimized point; by its strong tools include Selection, Cross-over and Mutation. This method requires a fitness function to obtain the next proper

generations by evaluating this function. The main disadvantage of this method is its slowness in convergence. Therefore, it is necessary to consider an experimental knowledge for the next generation. The algorithm is as follows:

1- The initial parameter search space is chosen with considering the information of the observer gain tuning section.

2- A desired sinusoidal input with a specified domain and frequency is determined. To do this, a series of simulations in various speeds are used, a voltage and current input are stored in memory and whenever the algorithm works, it uses one of these desired inputs. This method leads the algorithm to see the system dynamics. Each of these inputs has 60 points that determine a certain set of inputs.

3- For each set of inputs from stage 2, 50 number of population is selected for each of the 7 supposed coefficients. Each population is considered as a set of real numbers. Here, the coupling point can be selected only from the real numbers limit of each stage and by selecting randomly a real number from a proper interval; mutation performance will randomly change its value. Generation operator like the standard form performs each chromosome generation in respect of its criterion function G(θ).

4- After this stage, the target function $F(\theta)$ will be evaluated as follows. The coefficients k_1 to k_4 and k_ω which have the most effect considering the observer gain tuning section effect on system performance, will have a bigger weight on real function $G(\theta)$. Here, using the operators of the stage 3, the next generation will be produced.

5- The stages 2, 3 and 4 will be repeated over and over until the proper change of k_i the target function has an error lower than the given value or the maximum generation takes place.

The simulation Genetic algorithm has been developed according to the prescribed procedure with the following functions:

(82)
$$G(\theta) = \int \left(\sum_{i=1}^{5} (\tilde{a}_i - a_i)^2 + (\tilde{\omega} - \omega)^2 \right)$$

(83)
$$F(\theta) = \frac{1}{G(\theta) + \varepsilon}$$

(84)
$$\theta = [k_1, k_2, k_3, k_4, k_\omega, m_1, m_2]$$

Where ε is a small constant introduced to avoid overflow problems whenever F(θ) takes very small values. In this studied case, each reference consists of 60 points and the population number is set at 50 with probabilities $P_c = 0.85$ and $P_m = 0.05$.
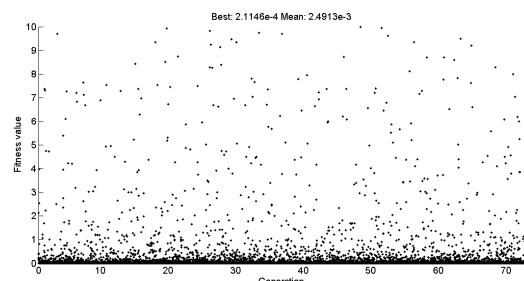

Fig. 4. Evolution of relative squared errors versus iterations.

In this state, the best solution will be obtained. The Fig.4. demonstrates the changes of parameters value k_i and m_i in respect of time. Considering the simulations, the resulted value for coefficients like k_i and m_i are presented in the Table 1.

Simulation results

To ensure the performance of observer and control system, the algorithm was simulated by the software Matlab/Simulink. Control method used in this paper is rotor flux in reference of synchronous. According to adjustment of the system gain and consideration the behavior of the components improved flux and current, coefficients k_i, m_1 and m_2 are obtained. Using the observer gain tuning section, modified current and flux components are estimated, and then motor torque is achieved. The Fig.5 illustrates the core losses are not considered, the speed of the induction motor will not reach its reference and there will always be a difference. This problem is more significant in lower speeds. In the Fig.5 we observe the changes in the speed of the induction motor in two states of considering the core losses and not considering. Next, algorithm performance is investigated. As you can see in the Table I, the highest gains are related to the tracking resistors and speed dynamic. It is related to the stator and rotor dynamics. In Fig.6 the variation of motor speed with changing of rotor resistance in the range 0.5pu to 1.5pu and magnetic inductance in the range 0.8 pu to 1.2 pu. is observed. In this case, variation of motor speed and torque are shown which are very fast. Fig. 7 shows the variation of stator three-phase current during simultaneous changes of rotor resistance and magnetic inductance. Considering to these Figures, observer performance accuracy related to the parameters change illustrated. Transient time for Classical FOC with consideration j=0.02 is in range 1 sec but, for proposed observer is in the range 0.3 sec. thus, the performance of proposed observer is faster the classical FOC.

Table 1 Values for coefficients

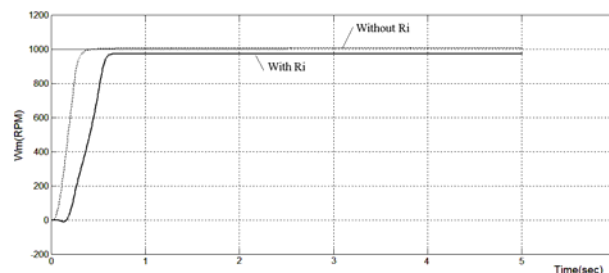| Symbol	Gain Value
k_1	1500
k_2	1.87
k_3	1.46
k_4	100
k_ω	12000
m_1	2
M_2	200

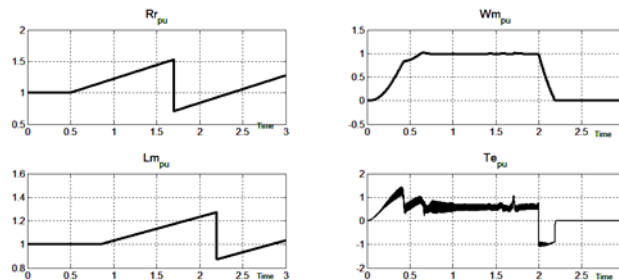Fig. 5. Evolution of Speed response with considering the core losses and not

Fig. 6. Speed step response with variation Rotor Resistance(pu) and magnetizing inductance(pu), motor speed(pu) and electromagnetic torque(pu).
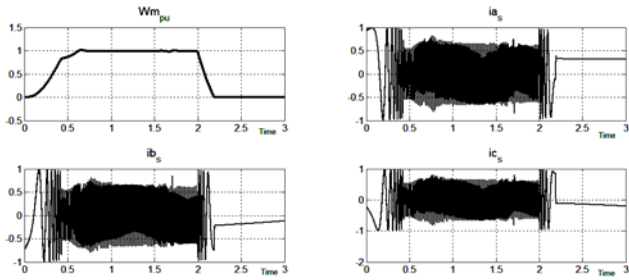
Fig. 7. speed and three phase stator current motor (pu) response with variation. Rotor Resistance and magnetizing inductance

One of main problems of the classical method FOC is in low speeds. There are two main reasons for weak performance of classical drives. First, the speed information is available at current and voltage, at zero speed, these values are close to zero and the system performance is reduced. The second reason is dead time. In most cases, the stator voltage is generated using pulse width modulation (PWM), which controls complementary transistor switching in a bridge circuit. The transistors should be switched complementarily. Simultaneously switching both transistors ON would cause a short-circuit connection, resulting in damage to power switching. That is why a short "dead time" when both transistors are switched OFF is inserted into the switching cycle. During the dead-time duration, the load inductance defines the voltage to keep inductive current flowing through diodes. The actual stator voltage then depends on the current direction. This is not too important for the control algorithm itself as it can be usually compensated by a current controller. Usually, when the load torque is constant, the worst error speed is less than 3%. This accuracy is acceptable in the most applications of induction motors serving. In this case the estimation of rotor resistance is very important and whatever this estimated effect is more precise, estimation of the speed is improving [21].

Fig. 8 and Fig. 9, illustrate speed, torque and three-phase stator current illustrate in the lower speeds, respectively. Nonlinear observer with the online parameter update has the accurate values of parameters at any time and speed. According to this fact, the control system can have a proper performance in a lower range of reference variations. As these Figures show, speed error is very low and desirable performance is achieved.
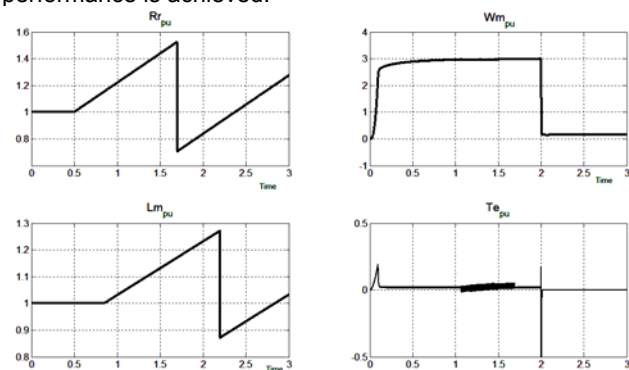

Fig. 8. Speed step response with variation of Rotor Resistance(pu) and magnetizing inductance (pu), motor speed(rpm) and electromagnetic torque (Nm) in low speed region.

Another important operational region for induction motor is the field weakening region. In this region by weakening the flux related to an inverse reference speed to nominal speed ratio, motor speed will be higher than nominal speed. Fig.14 and Fig.15 show changes in motor speed, motor torque, as well as changes in the three-phase stator while

rotor resistance and magnetic inductance change. In this case, maximum speed error is less than 3% of reference speed. The good performances of nonlinear observer and drive have been achieved.
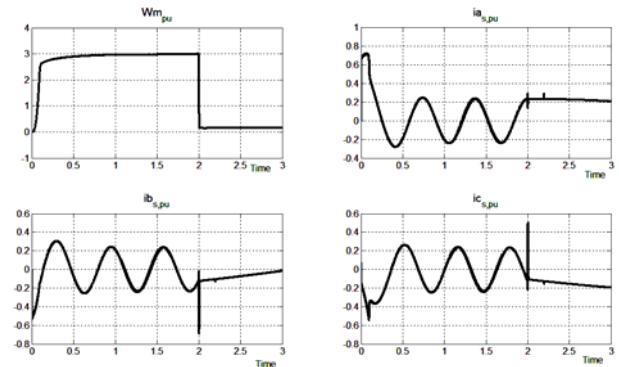

Fig. 9. speed(rpm) step response and three phase stator current motor (A) in low speed region with variation. Rotor Resistance and magnetizing inductance
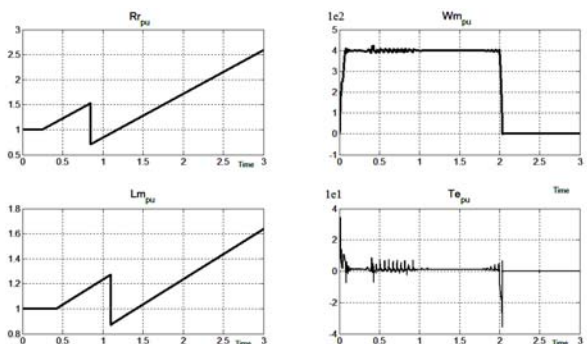

Fig. 10. Speed step response with variation of Rotor Resistance(pu) and magnetizing inductance(pu), motor speed(rpm) and electromagnetic torque(nm) in Field Weakening region
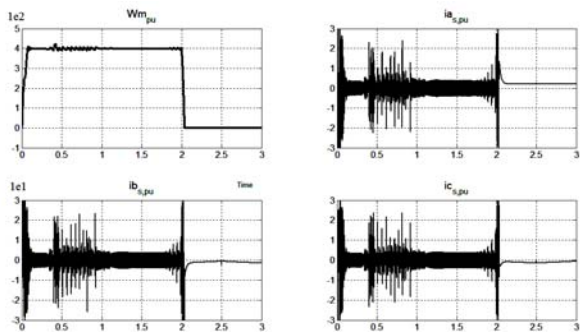

Fig. 11. Speed(rpm) and three phase stator current motor (A) response in field weakening region with variation of Rotor resistance and magnetizing inductance.
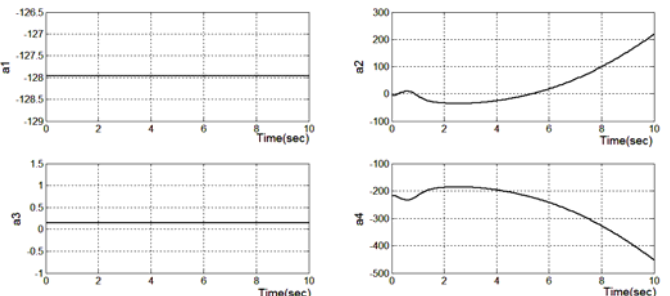

Fig. 12. a1, a2, a3 and a4 -parameter adaptation.

Fig. 12 shows a_i respect to time by the stator and rotor resistance changing. In this Figure, after a short time, a_1 values converge to final values. Then, a proper

performance can be expected from the control system. The next simulation is executed to examine the proposed observer behavior during load-torque change. The motor is started with nominal load torque. Then, the load-torque is changed to 1 N.m which introduced at time 2sec, and returned to 0 at time 5 s. As it can be seen in Fig. 13, the rotor speed changes for a short time until the control algorithm compensates the load torque. However, even in this situation, there is only a little error in the speed estimate.

Fig. 14 shows the torque and stator current behaviors when the torque and speed are adjusted to 0.2p.u. and 0.8p.u., respectively. The simulation result in Fig. 14 proves that, in the moderate speed, the stator current is sinusoidal with small distortion, while the torque follows its final reference value.
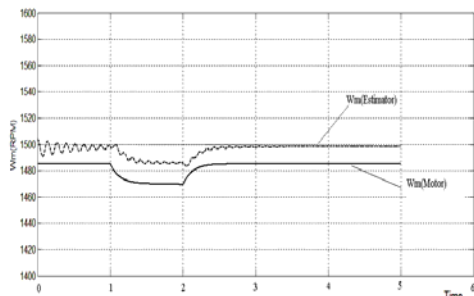
Fig. 13. Comparison of real rotor speed (solid) and estimated value (dashed) during load-torque change.

Fig. 15 shows both torque and stator current responses for the low rotor speed and a step change from 0.2 to 0.4 in torque reference. The presented results show that the response time of torque, for this step excitation, is equal to 1ms, and torques settles within this time.
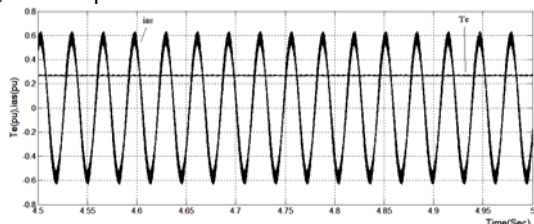

Fig. 14. Estimated torque and stator current for the speed set to 0.8 p.u. and torque set to 0.2 p.u.
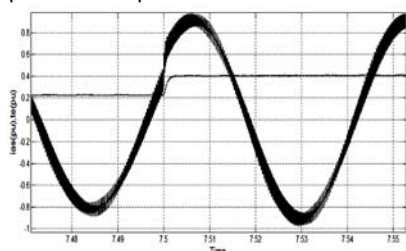

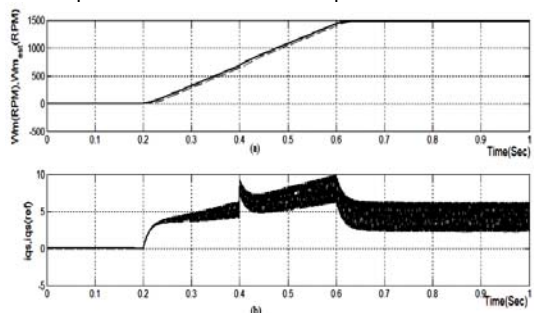Fig. 15. Torque and stator current responses for low speed reference step excitation from 0.2 to 0.4 p.u

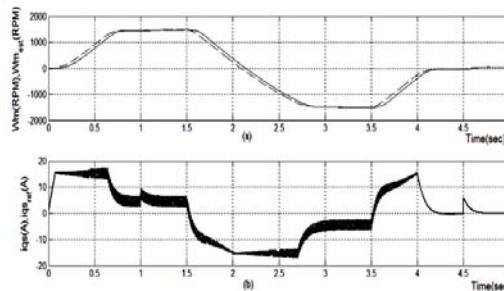Fig. 16. Speed and current responses for speed reference step excitation from 0 to 1 p.u.

Fig. 17. Speed and current responses for speed reference step excitation from -1 to 1 p.u.

Fig. 16(a) shows the measured and estimated speed when its reference changes from 0 to 1 p.u. This figure also concluded the current response. Fig. 17 shows the speed and the current when the measured speed is controlled in the four-quadrant operation region. The base speed is 1500 (rpm). Fig. 17 shows the four-quadrant operation characteristics of the proposed method. It is seen that the current control is somewhat unstable close to 0 [rpm]. However, it is also seen that the speed is well regulated in transients by the proposed method.

Experimental results

The setup comprises the three-phase VSI with Insulated-Gate Bipolar Transistors (IGBTs). The stator voltage commands are modulated by using symmetrical PWM, constant switching frequency 4 kHz. Dc bus voltage of the VSI is 540V, with the VSI overcurrent protection set to 50 A. The PWM modulation and stator currents sampling are realized by using a custom field-programmable gate-array (FPGA)-based hardware, with measurement executed by using the 12-b resolution. The stator current signals are, four analog-to-digital (A/D) conversions, filtered by using a first-order filters having the bandwidth set to 25 kHz. The currents are sampled at the instances in the middle of the symmetric PWM cycle in order to minimize the ripple component in the stator current measurements. The sampling period is set to 200us. The nonlinear algorithm is implemented on a DSP TMS320VC5416, running the real-time control hardware with the floating-point arithmetic precision. The induction machine under test was coupled to a separately controlled dc machine used as a dynamic brake. The steady-state and transient behavior of the drive were investigated through various sets of experimental tests.

A. Steady-State Operating Conditions

The investigation of drive behavior in the steady state is necessary in order to determine the following drive characteristics: the stability of drive operation, torque ripple in the steady state, and speed steady-state error. The investigation of these characteristics enables the comparison of the outlined strategy with the existing FOC strategies. The steady-state behavior is investigated in the different operating conditions (e.g., for the low, mid- and high-speed regions).

The drive behavior in operating conditions with low speed was examined. Fig. 18 shows the current and torque behaviors for the locked rotor with the rotor flux and torque set to their rated values.

Since the motor is operated in low speed, the drive operates in the range of low frequencies. Generally, the sensorless IM control strategies exhibit the deterioration of operation performance at low field frequencies. In this case, the voltage fundamental is very small and comparable with the level of voltage distortions exhibited by VSI, which may cause the unsuitable speed estimation. The investigations

presented in Fig. 18 show that the drive operation is stable, without nonlinear distortions of the stator current.

Fig. 19 shows the torque and stator current behaviors for the torque set to 0.2 p.u. and speed set to 0.8 p.u. The experimental results in Figs. 16 and 17 prove that, in the mid- speed and high-speed region, the stator current is sinusoidal with small distortions, while the torque matches its reference value. The presented results also prove that the drive operates stably and accurately in the steady state within a wide range of rotor speeds.
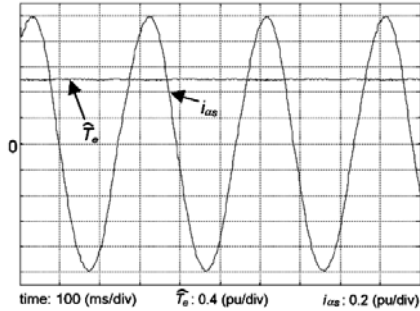

Fig. 18. Estimated torque and stator current for the low speed($\widehat{T}_e = 0.4(pu / div)$ and ias=0.2(pu/div)).
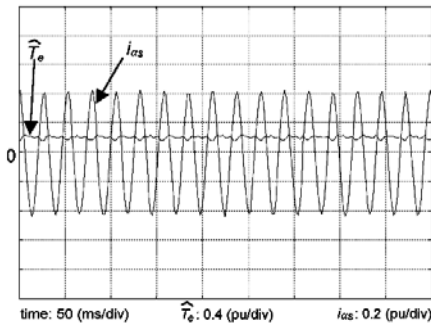

Fig. 19. Estimated torque and stator current for the speed set to 0.8 p.u. and torque set to 0.2 p.u. ($\widehat{T}_e = 0.8(pu / div)$ and ias=0.2(pu/div)).

B. Transient Operating Conditions

The transient behavior of the proposed nonlinear algorithm was investigated for low-speed, mid-speed and filed weakening regions. The transient experimental tests are necessary to investigate the dynamics of the observer.

Fig. 20 shows torque and stator current responses for the low rotor speed and torque reference step change from 0.2 to 0.4 p.u. The presented results show that the response time of torque, for the step excitation, is equal to four to five sampling periods, while the settling time is with the zero steady-state error. This test shows that the proposed FOC algorithm has a response time comparable to those achieved with the basic FOC algorithms. Moreover, even though the basic FOC strategies exhibit the response times of one to two sampling periods, they can hardly meet requirements for the stable operation and low torque and speed, ripple in all operating conditions. The traces of Fig. 21 represent the torque response on the step excitation, for the rotor speed set to 0.5 p.u. The presented test results prove that the proposed nonlinear algorithm is robust in relation to rotor speed variations. Fig. 22(a) shows the measured speed and estimated speed when speed change from 0 to 1 p.u. Fig. 22(b) shows the current when speed changes. Fig. 25 shows the speed and the current when the measured speed is controlled and used for field weakening operation. The base speed is 1500 (rpm). Fig. 23(a) show the estimated speed and measured speed. Fig. 23(b) shows that the q-axis current is well regulated. Fig. 24 shows the four-quadrant operation characteristics of the

proposed method. It is seen that the current control is somewhat unstable close to 0 [rpm]. However, it is also seen that the speed is well regulated in transients by the proposed method.
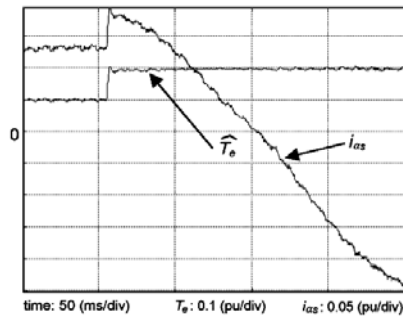

Fig. 20. Torque and stator current responses for low speed reference step excitation from 0.2 to 0.4 p.u.
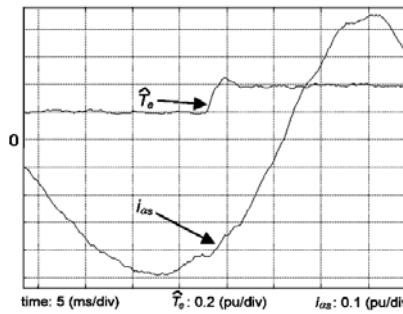

Fig. 21. Torque and stator current responses for speed set to 0.4 p.u. and for torque reference step excitation from 0.2 to 0.4 p.u.

The next experiment was aimed to consider the observer behavior during load-torque change. The motor has started its operation with zero load torque. Then, the load-torque is changed to 1 N·m after 3 seconds, and returned to 0 after 7 seconds. As it can be seen in Fig. 25, the rotor speed is changed for a short time until the control algorithm compensates the load torque. However, even in this situation, there is only a little error in the speed estimation
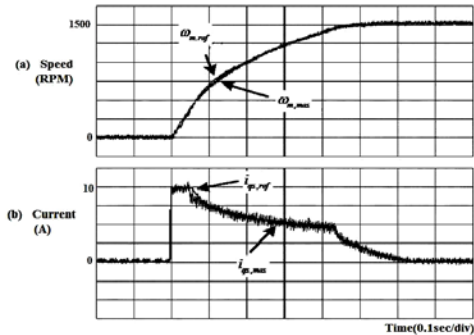

Fig. 22. Speed and current responses for speed reference step excitation from 0 to 1 p.u.
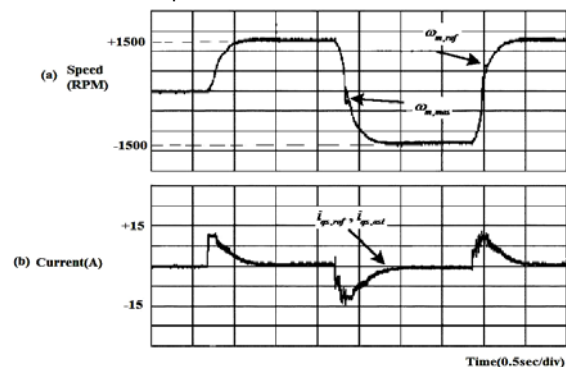

Fig. 23. Speed and current responses for speed reference step excitation from -1 to 1 p.u.
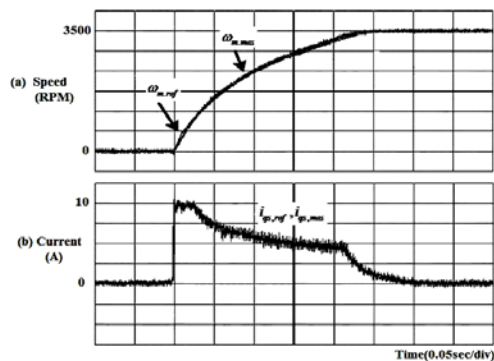
Fig. 24. Speed and current responses for field weakening operation. from 0 to 3500 Rpm
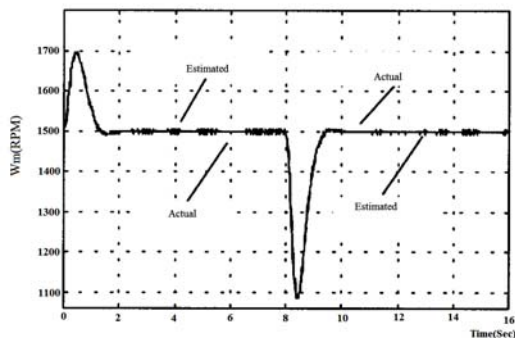

Fig. 25. Comparison of real rotor speed (solid) and estimated value (dashed) during load-torque change.

Conclusion

In this paper, an improved sensor-less rotor-flux oriented vector-control technique for using an induction motor drive is proposed. By taking advantages of a non-linear observer algorithm, the rotor speed can be tracked even in the case of rapid torque changes as much as motor parameters. The simulation results and experimental results show a good improvement in the speed control ranges of a real ac induction machine based on the classical rotor-flux-oriented vector control.

   The non-linear observer can estimate both the rotor speed and motor parameters simultaneously while two control estimator units should be utilized in the previous methods. Also a very good robustness in the speed and torque load changes are obtained according to the simulation and experimental results. Furthermore, the higher accuracy especially in the low speeds is one of the prominent points in this method compared to the others in the literature. In addition the proposed method is cost-efficient as there is no need for flux and speed sensors at all. The algorithm can be applied to the other control methods because of its independence to the control scheme. In addition, with appropriate adjustment of dynamic rotor we will have very good responses.

Appendix
Motor data: Rs = 1.6 Ώ, Rr = 1.2 Ώ, Lm = 52 mH, Ls = 53 mH, Lr = 53 mH,

REFERENCES
[1] Kouki Matsuse, Shotaro Taniguchi, Tatsuya Yoshizumi, and Kazushige Namiki," A Speed-Sensorless Vector Control of Induction Motor Operating at High Efficiency Taking Core Loss into Account", IEEE TRANSACTIONS ON INDUSTRY APPLICATIONS, VOL. 37, NO. 2, MARCH/APRIL 2001.
[2] Jia-jun WANG, Jie HE, "Torque and flux direct backstepping control of induction motor", the 7th World Congress on Intelligent Control and Automation June 25 - 27, 2008, Chongqing, China.
[3] Epaminondas D. Mitronikas and Athanasios N. Safacas, Member, IEEE," An Improved Sensorless Vector-Control Method for an Induction Motor Drive", IEEE TRANSACTIONS ON INDUSTRIAL ELECTRONICS, VOL. 52, NO. 6, DECEMBER 2005.
[4] Epaminondas D. Mitronikas and Athanasios N. Safacas, Member, IEEE, "An Improved Sensorless Vector-Control Method for an Induction Motor Drive," IEEE TRANSACTIONS ON INDUSTRIAL ELECTRONICS, VOL. 52, NO. 6, DECEMBER 2005.
[5] J. Holtz and Q. Juntao, "Sensorless vector control of induction motors at very low speed using a nonlinear inverter model and parameter identification," IEEE Trans. Ind. Appl., vol. 38, no. 4, pp. 1087–1095, Jul./Aug. 2002.
[6] Maurizio Cirrincione, Marcello Pucci, Giansalvo Cirrincione, and Gérard-André Capolino, "Constrained Minimization for Parameter Estimation of Induction Motors in Saturated and Unsaturated Conditions," IEEE TRANSACTIONS ON INDUSTRIAL ELECTRONICS, VOL. 52, NO. 5, OCTOBER 2005.
[7] Marcello Montanari, Sergei M. Peresada, Carlo Rossi, and Andrea Tilli, "Speed Sensorless Control of Induction Motors Based on a Reduced-Order Adaptive Observer," IEEE TRANSACTIONS ON CONTROL SYSTEMS TECHNOLOGY, VOL. 15, NO. 6, NOVEMBER 2007
[8] C. Shauder, "Adaptive speed identification for vector control of induction motors without rotational transducers," IEEE Trans. Ind. Appl., vol. 28, no. 5, pp. 1054–1061, Sep./Oct. 1992.
[9] C. Lascu, I. Boldea, and F. Blaabjerg, "A modified direct torque control for induction motor sensorless drive," IEEE Trans. Ind. Appl., vol. 36,no. 1, pp. 122–130, Jan./Feb. 2000.
[10] H. Kubota, I. Sato, Y. Tamura, K. Matsuse, H. Ohta, and Y. Hori, "Stable operation of adaptive observer based sensorless induction motor drives in regenerating mode at low speeds," in Conf. Rec. IEEE-IAS Annu.Meeting, vol. 1, Oct. 2001, pp. 469–474.
[11] G. Guidi and H. Umida, "A novel stator resistance estimation method for speed-sensorless induction motor drives," IEEE Trans. Ind. Appl., vol. 36, no. 6, pp. 1619–1627, Nov./Dec. 2000.
[12] H. Kubota, I. Sato, Y. Tamura, H. Ohta, and Y. Hori, "Stable operation of adaptive observer based sensorless induction motor drives in regenerating mode at low speeds," IEEE Trans. Ind. Appl., vol. 38, no. 4, pp. 1081–1086, Jul./Aug. 2002.
[13] H. Sugimoto, "One improving measures of stability in regeneration operation of speed sensorless vector control induction motor system using adaptive observer of secondary magnetic flux," in Proc. Int. Power Electronics Conf. (IPEC), Tokyo, Japan, 2000, vol. 3, pp. 1069–1074.
[14] H. Tajima, G. Guidi, and H. Umida, "Consideration about problems and solutions of speed estimation method and parameter tuning for speedsensorless vector control of induction motor drives," IEEE Trans. Ind. Appl., vol. 38, no. 5, pp. 1282–1289, Sep./Oct. 2002.
[15] Surapong Suwankawin and Somboon Sangwongwanich, "Design Strategy of an Adaptive Full-Order Observer for Speed-Sensorless Induction-Motor Drives—Tracking Performance and Stabilization", IEEE TRANSACTIONS ON INDUSTRIAL ELECTRONICS, VOL. 53, NO. 1, FEBRUARY 2006.
[16] K. Shi, T. Chan, Y. Wong, and S. Ho, "Speed estimation of an induction motor drive using an optimized extended Kalman filter," IEEE Trans. Ind. Electron., vol. 49, no. 1, pp. 124–133, Feb. 2002.
[17] B. Peterson, "Induction machine speed estimation, observations on observers," Ph.D. dissertation, Dept. Ind. Elect. Eng. Autom., Lund Inst. Technol., Lund, Sweden, 1996.
[18] H. Kubota, K. Matsuse, and T. Nakano, "DSP-based speed adaptive flux observer of induction motor," IEEE Trans. Ind. Appl., vol. 29, no. 2, pp. 344–348, Mar./Apr. 1993.
[19] Pavel Vaclavek, and Petr Blaha, Lyapunov-Function-Based Flux and Speed Observerfor AC Induction Motor Sensorless Control and Parameters Estimation," IEEE TRANSACTIONS ON INDUSTRIAL ELECTRONICS, VOL. 53, NO. 1, FEBRUARY 2006.
[20] Giovanni Bottiglieri, Student Alfio Consoli, and Thomas A. Lipo, Life" Modeling of Saturated Induction Machines With Injected High-Frequency Signals," IEEE TRANSACTIONS ON ENERGY CONVERSION, VOL. 22, NO. 4, DECEMBER 2007.
[21] Faa-Jeng Lin, Senior Member, IEEE, Rong-Jong Wai, Member, IEEE, Wen-Der Chou, and Shu-Peng Hsu," Adaptive Backstepping Control Using Recurrent Neural Network for Linear Induction Motor Drive", IEEE TRANSACTIONS ON INDUSTRIAL ELECTRONICS, VOL. 49, NO. 1, FEBRUARY 2002
[22] J.-W. Kim and S. W. Kim, "A novel parametric identification method using dynamic encoding algorithm for searches (DEAS)," in Proc. Int.Conf. Control, Automation and Systems, Oct. 2002, pp. 406–411.
[23] K. L. Shi, T. F. Chan, Y. K. Wong, and S. L. Ho, "Speed estimation of induction motor using extended Kalman filter," in Proc. IEEE WinterMeeting 2000, vol. 1, Singapore, Jan. 23–27, 2000, pp. 243–248.

Mehdi ALEMI-ROSTAMI, Adib ABRISHAMIFAR
Iran University of Science and Technology (IUST) (1), Iran University of Science and Technology (IUST) (2)